Progress in Organic Coatings 130 (2019) 8–16

Contents lists available at ScienceDirect

Progress in Organic Coatings

journal homepage: www.elsevier.com/locate/porgcoat

Facile preparation of high solid content waterborne polyurethane and its application in leather surface finishing

Yanting Han[a], Jinlian Hu[a,*], Zhongyin Xin[b]

[a] Institute of Textiles & Clothing, The Hong Kong Polytechnic University, Hung Hom, Kowloon, 999077, Hong Kong, China
[b] National Engineering Laboratory for Clean Technology of Leather Manufacture, Sichuan University, Chengdu, Sichuan, China

ARTICLE INFO

Keywords:
Waterborne polyurethane
High solid content
Coatings
Leather
Surface finishing

ABSTRACT

High sold content waterborne polyurethanes (WPUs) were prepared based on star-shape prepolymer which was synthesized via arm-first approach using pentaerythritol (PE) as core. With PE content increasing from 0.3% to 1.2%, WPU dispersions presented a decreasing trend in average particle size, whilst size distribution transited from bimodal distribution to monomodal distribution. This may contribute to variation of surfaces roughness of coatings during film formation process. Infrared spectra and atomic force microscope revealed micro-phase separation structure within WPU coatings and hydrogen-bond interactions between soft segments and hard segments. Water swelling ratios of WPU coatings were below 17% and their swelling behaviors were consistent with kinetic first-order equation. Moreover, WPU coatings showed excellent thermal stability and mechanical properties with elongation at break of 400% and breaking strength reaching 15 MPa. It was found that WPU coatings possess optimum damping properties at 50 °C which can be regulated by PE content. Notably, application of high solid content WPU dispersions on leather surface resulted in excellent comprehensive performance, implying the potential application of WPU dispersions as leather finishing agents.

1. Introduction

The restrictive environmental regulations regarding volatile organic chemicals (VOCs) stimulate increasing research and development of waterborne polymers for various applications during these years [1,2]. As one of branch of multifunctional coatings, waterborne polyurethane (WPU) has been drawing much attention both in academic and industry fields because of its less organic compound and non-toxicity compared with conventional solvent based PU [3,4]. Apart from the environmental advantages, WPU present other outstanding physicochemical properties including good elasticity, excellent mechanical strength, reasonable biological performance and high adhesiveness [5,6]. All these features conduce to applications of WPU on a wide range of fields, such as coatings, adhesives and finishing agents [7,8]. Nevertheless, due to high latent heat of evaporation of water, WPU leads to inferior drying rates and high cost for packaging and transportation. Hence, it is significant and urgent to improve solid content of WPU for application, especially in areas where WPU are used in large quantities, such as leather industry which requires surface finishing to provide product with glossy, fastness, durability, hand feeling, etc [9]. Moreover, leather products including clothes, shoes and bags are in direct contact with human skin during use, so it is especially important to use green and non-toxic finishing agents. Therefore, non-pollution and high value-added waterborne leather finishing agents with outstanding overall performance are supposed to bring profound significance for development of leather industry.

The key point for preparation of WPU is to effectively disperse polyurethane prepolymers into water to form a stable colloidal dispersion, which involves a phase inversion of PU-water system from w/o to o/w [10,11]. Hence, to facilitate the inversion efficiency can help to reduce the dosage of water, thereby improving solid content of WPU. The strong interactions between the colloidal particles would increase with augment of solid content, leading to the high viscosity of WPU, thus, controlling the viscosity of latex also accounts for the difficulties to prepare WPU with high solid content [12,13]. Lee et al. [10] incorporated ionic groups at the flexible chain ends of PU to improve mobility and exposure of ionic groups on particle surface, obtaining a WPU with up to 45% solid content. They presented that the low content of ionic group suppresses swelling of latex particles caused by electric double layer and electroviscous effect, leading to decreased viscosity of WPU. However, there is research which claimed that 2% ionic groups are essential for stability of high solid content WPU [14,15]. Nevertheless, efforts has been paid to use nonionic monomer to help reducing the dosage of ionic groups and decreasing viscosity due to its synergistic

* Corresponding author.
E-mail address: jinlian-hu@polyu.edu.hk (J. Hu).

https://doi.org/10.1016/j.porgcoat.2019.01.031
Received 16 November 2018; Received in revised form 28 December 2018; Accepted 16 January 2019

effect on improving the stability of WPU [11].

On the other hand, particle size distribution also plays important role in increasing solid content of latex. It is claimed that small particles can fit into the voids among the large ones, thus increasing the maximum packing factor of particles [16]. Peng et al reported that solid content of WPU were improved to 55% with bimodal particle size distribution by using WPU with large particle size to emulsify the more hydrophilic WPU which can be dispersed into smaller particles [17]. However, the broad particle size distributions may lead to the instability of WPU. Although these literatures reported the achievement of high solid content of WPU either by molecule design or process optimization, they were unavoidably used organic solvent, such as acetone, to decrease the viscosity of prepolymer resulted from its increasing entanglements and hydrodynamic volumes. And the organic solvents also need to be removed from the obtained WPU dispersions by vacuum distillation [11,13,17]. Thus, it can be seen the conventional synthesis of WPU dispersions still involves release of VOCs more or less.

The star-shaped polymer is a type of branched polymer with special architecture containing at least three linear polymeric chains of comparable lengths which radiate from one single multifunctional branched core [18–23]. This structure endows star-shaped polymer with specific space configuration including small radius of gyration and hydrodynamic volume, which in turn affects the physiochemical properties of micellization in aqueous solution [19]. Compared with the linear analogues of identical molar masses, star-shaped polymer has advantages, such as better solubility, low viscosity and facile functionality of the terminal groups [22,24]. Therefore, introducing special topological structure into polyurethane architecture may provide a green approach to realize the easier dispersion of hydrophilic polyurethane into water phase without aiding of toxic solvent. Moreover, the increased crosslinking rate of the star shaped polyurethane may lead to compact structure of cured coatings, resulting in enhanced toughness, which can broaden WPU application on specific areas, such as marine antifouling [23]. There were some researches of star shaped PU, However, they were either solvent-based or used specific monomers which need extra synthesis under harsh conditions [20,19–23,25]. Wang et al [21] used pentaerythritol as the core to synthesize star-shaped polyurethane. It is found that star-shape polyurethane can self-assemble to form micelles in water, which benefits improving high solid content of WPU. However, in their study, aggregations also occurred during dispersion process even under pre-dissolving in tetrahydrofuran. This is due to low hydrophilicity of polyurethane with ionic hydrophilic groups. Additionally, only drug delivery properties of stared-polyurethane micelles were investigated in their research. Hence, more performances and applications of star-shaped WPU remains to be studied.

In this study, a four arms star-shaped polyurethane prepolymer based on pentaerythritol as core was synthesized via “arm first” approach. Polytetrahydrofuran ether diol (PTMG) was choose as soft segment while isophorone diisocyanate (IPDI) were selected as hard segment. Dimethylol propionic acid (DMPA) and ethoxylated polymer diol (N-120) were incorporated as composite hydrophilic groups for enhanced hydrophilic efficiency of polyurethane molecular. As expected, 45% solid content of waterborne polyurethane (WPU) dispersions were obtained without aiding of organic solvent. Such new system realizes a facile solvent-free preparation of high solid content waterborne polyurethane with high performance. Particles size distribution, viscosity and stability of the WPU dispersions were analyzed. The surface topography, phase structure, thermal and mechanical properties of the derived coatings were also studied. Moreover, high sold content WPU dispersions was applied on surface of leather for finishing for the first time. The performances of finished leather were evaluated to verify the applicability of WPU dispersions in leather industry. The main objective of the work was to explore a green facile method to prepare high solid content WPU, as well to reveal the relations between structure and properties for its potential applications.

2. Experimental

2.1. Materials

Polytetramethylene glycol (PTMG, M_w = 1000 g/mol), Dimethylol propionic acid (DMPA), pentaerythritol (PE), and a linear difunctional polyethylene glycol monomethyl ether (Ymer™ N120) were purchased from Sweden Perstorp. Isophorone diisocyanate (IPDI) was supplied from Bayer, Germany. Dibutyltin dilaurate (DBTDL), triethylamine (TEA) and ethylenediamine (EDA) were obtained from Chengdu KeLong Chemical Industry Co., Ltd of China. DBTDL was used as received. PTMG was dried and degassed at 110 °C under vacuum for 2 h. DMBA and PE were dried at 70 °C for 48 h in vacuum oven. Double-distilled water was used throughout. Unfinished leather was provided by Guangzhou Honggu Leather Articles Co., Ltd of China.

2.2. Preparation of WPU dispersions

The polymerization was carried out in a flask equipped with a mechanical stirrer, thermometer, reflux condenser and additional funnels under a constant temperature oil bath. PTMG, nonionic hydrophilic monomer (N120) and DMPA were added to the flask. After mixing evenly, IPDI was added followed by addition of 0.05 wt % of DBTDL drop by drop. The mixtures were reacted at 85 °C for 3 h to obtain polyurethane prepolymer (NCO/OH = 2.17). PE was then added for chain extension for another 2 h. The resulted star shaped prepolymer was then neutralize by TEA for 15 min at 40˜45 °C. Quantitative distilled water was subsequently added rapidly with stirring at an agitation speed of 2000 rpm for 10 min. EDA was added dropwise. This chain extension reaction at 35 °C was lasted for 1.5 h. The final obtained WPU dispersion had ˜45 wt.% solid content and pH value of 7. Coating specimens were prepared by casting the dispersions onto glass plates. They were firstly dried at ambient temperature for 12 h, and then at 60 °C for 24 h. The thickness of obtained films was about 0.4 mm. Formula of WPU dispersions were summaries in Table 1 and procedure is shown in Fig. 1(a).

2.3. Characterizations

Particle size distribution of WPU dispersions was tested by using particle size analyzer (Zetasizer Nano S90). The viscosities of WPU dispersions were measured on NDJ-8S digital readout viscometer at 25 °C with a rotate speed of 30 rpm. Morphology of WPU dispersion particles were characterized by Transmission electron microscopy

Table 1
Formula of WPU dispersions.

Code	Dosage (molar)								Solid content (%)
	PTMG-1K	PTMG-2K	DMPA	N120	PE	IPDI	TEA	EDA	
WPU-0.3	0.0450	0.0225	0.1380	0.0120	0.0034	0.2000	0.0100	0.0740	45.04%
WPU-0.6	0.0450	0.0225	0.1380	0.0120	0.0068	0.2000	0.0100	0.0680	46.52%
WPU-0.9	0.0450	0.0225	0.1380	0.0120	0.0100	0.2000	0.0100	0.0620	45.54%
WPU-1.2	0.0450	0.0225	0.1380	0.0120	0.0134	0.2000	0.0100	0.5500	45.30%

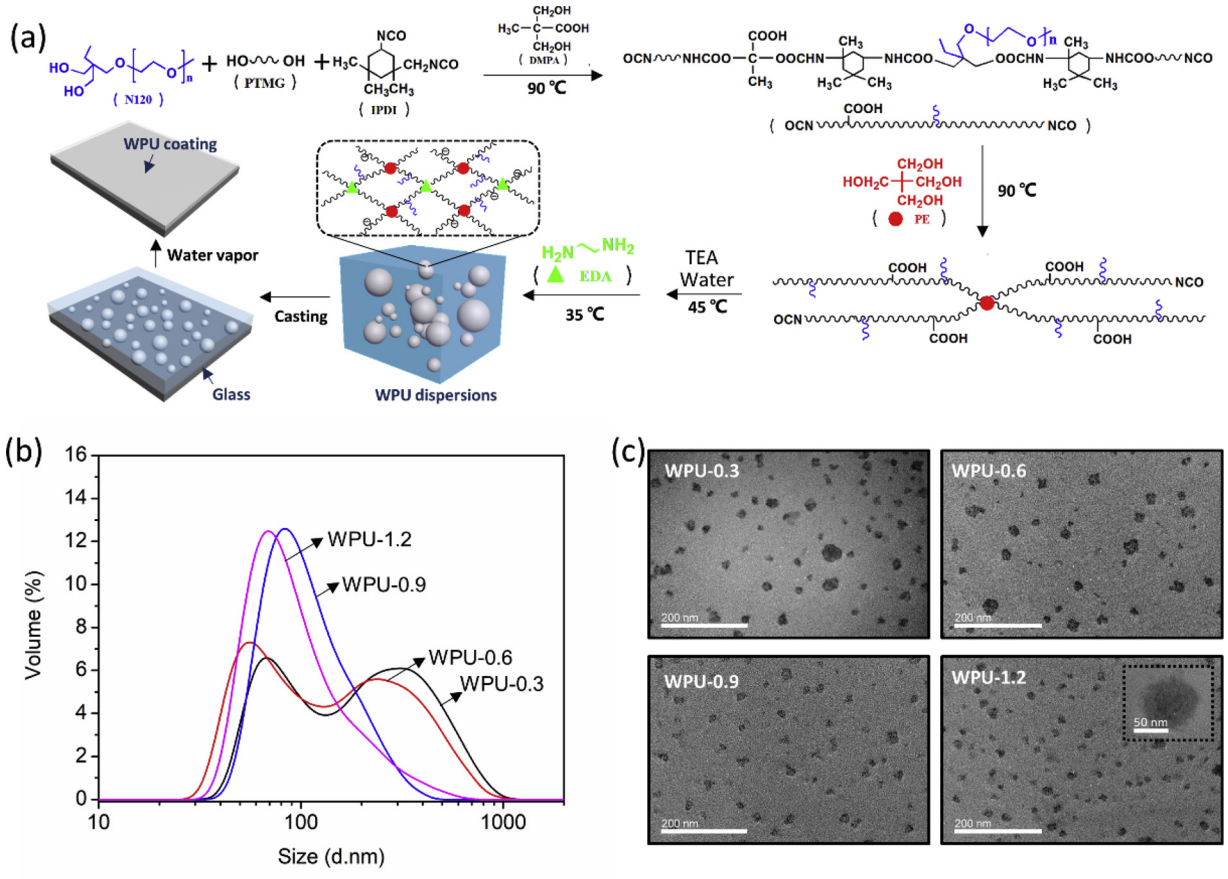

Fig. 1. (a) Scheme illustration for preparation of WPU dispersions and coating; (b) particle size distribution of WPU dispersion; (c) TEM photos of WPU dispersions.

(JOEL,Peabody, MA, USA) operating at an accelerating voltage of 200 kV. The WPU dispersions were diluted to a concentration of 1 wt% and were drop on a copper mesh for TEM observation. Fourier transform infrared (FTIR) spectra of the coatings were performed on a NEXUS 670 spectrophotometer (Thermo Fisher Scientific, USA) in transmission mode. Atom force microscopy (AFM) was performed on the surface of the coatings with a scanning area of 5 μm × 5 μm using the SPA-400 Atomic force microscope (Seiko Instruments Inc. Japan) in tapping mode. Roughness analysis was carried out using NanoScope-Analysis software. To measure swelling in water, dried coatings (weight designated as m_0) was immersed in water for 70 min at 25 °C, the weight of the samples were measured (m_i) at certain time interval. Swelling ratio was measured by the equation of Swelling ratio (%) = $(m_i - m_0)/m_0 \times 100\%$. Thermogravimetric analysis (TGA) was carried out in TG 209 F1 differential thermogravimetric analyzer (NETZSCH Instruments, Germany) at a heating rate of 10 °C /min from 100 °C to 550 °C under nitrogen atmosphere. Dynamic viscoelastic behaviors of samples (5 × 10 mm) were investigated using DMA 242 C analyzer (NETZSCH Instruments, Germany) from -100 °C to 150 °C with a heating rate 5 °C /min at 1 Hz. Mechanical properties of coatings with a size of 5 × 25 mm was measured using tensile testing machine (GT-AI-7000S) with elongation rate of 100 mm/min under ambient conditions. The mechanical properties of finished leather (5 × 15 mm) were also investigated with elongation rate of 50 mm/min. The surface structure and cross section of finished leather samples were characterized by JEOL-6490 SEM. Samples were sprayed gold for testing. Water contact angle on leather samples were evaluated using the OCAH200 high-speed video contact angle measurer (DataPhysics Instruments GmbH Ger, Filderstadt, Germany).

3. Results and discussions

3.1. Size distribution and morphology of high solid content WPU dispersions

The particle size distribution of WPU dispersions are shown in Table 1. With increasing PE content, average particle size decreases from 205.9 nm to 111.9 nm, accompanied with particle size distribution index (PDI) decreases from 0.325 to 0.175. It can be seen from Fig. 1(b) that WPU-0.3 and WPU-0.6 have a bimodal particle size distribution. By increasing PE content, volume fraction of colloidal particles with large particle size gradually decrease while particles with small particle size increase. As a result, particle sizes of WPU-0.9 and WPU-1.2 exhibit a monomodal peak distribution, implying that their particle size distribution become narrower. This is because PU prepolymer crosslinked by PE has a “star-shape” structure [21]. That means the number of PU molecules with branch arms increases. Such branched structure is compact and is not easy to undergo inter-molecular entanglement [21,23]. Hence, during dispersion process, prepolymers molecules can be easily emulsified without condensation, so that the average particle size reduced whilst particle size distribution narrowed. Besides, viscosity of WPU dispersions increased with PE content (Table 2), which may because overall interaction force between particles are enhanced. The structure and morphology of WPU dispersion particles were identified by TEM. Due to dehydration process, particle size observed from TEM were smaller than the results obtained from particle size analyzer. It can be seen that for all samples, WPU particles are well dispersed without obvious aggregation. Notably, large particles can be observed in WPU-0 and WPU-0.3. Nevertheless, with increasing PE content, large particles disappeared whilst size distribution become uniform, which consists with results obtained from particle size analyzer. Moreover, the WPU dispersions has no delamination or gel after storage for 6 months

Table 2
Emulsion properties of high solid content WPU dispersions.

	PE content (%)			
	0.3	0.6	0.9	1.2
Average particle size /nm	205.9	177.6	131.9	120.1
PDI	0.325	0.249	0.234	0.185
Viscosity /mPa·s	6	28	45	64
Storage stability	> 6 months	> 6 months	> 6 months	> 6 months

at room temperature, indicating their good storage stability.

3.2. Structure and surface morphology of coatings formed by high solid content WPU dispersions

The infrared spectra of PE and WPU coating samples are shown in Fig. 2(a). It is reported that free −OH groups on PE exhibit stretching vibration bands at 3590-3650 cm^{-1} [26]. In this study, characteristic bands of −OH groups on spectrum of PE shift to lower wavenumber (3100-3550 cm^{-1}), indicating that the −OH have formed internal hydrogen bonds. During synthesis of WPU, high temperature will lead to disconnection of these internal hydrogen bonds, releasing free −OH groups on PE which can participate reactions with -NCO. It can be seen that the distinct peaks for free hydroxyl groups disappeared on spectra of WPU-0.6 and WPU-1.2. In addition, characteristic peak of -NCO at 2275 cm^{-1} were not observed, indicating the completely reactions of isocyanate. On spectra of all WPU coating samples, strong vibration peaks of N−H (3341 cm^{-1}), $-CH_2$ (2921 cm^{-1}) and $-CH_3$ (2858 cm^{-1}), as well as characteristic peaks of C−O−C (1108 cm^{-1}) and -C = O (1716 cm^{-1}) from soft segments are found [5,27,28]. Besides, there is stretching vibration peak at 1245 cm^{-1}, which attributes to C−O−C from -NHCOO- [27]. These results confirm the polyurethane molecular structures. FTIR can be used to study hydrogen bonding behavior of polyurethane which relate to its microphase separation structure [28]. Particularly, hydrogen bonds are formed between -NH groups in hard segments and C═O groups from both hard and soft segments. Since soft segment based on polyether glycol has no C═O groups, it is seasonable to investigate hydrogen bonds within hard segment according to spectra in C═O stretching region [29]. As shown in Fig. 2(b), peak fitting methods [30] was applied to obtain three characteristic peaks which are attributed to C═O with non-hydrogen bonding (1724 cm^{-1}), disordered hydrogen bonding (1700 cm^{-1}) and ordered hydrogen bonding (1660˜1630 cm^{-1}) respectively [31]. It can be seen that peaks of bonded C═O are much stronger than that of free C═O in WPU-0.3,

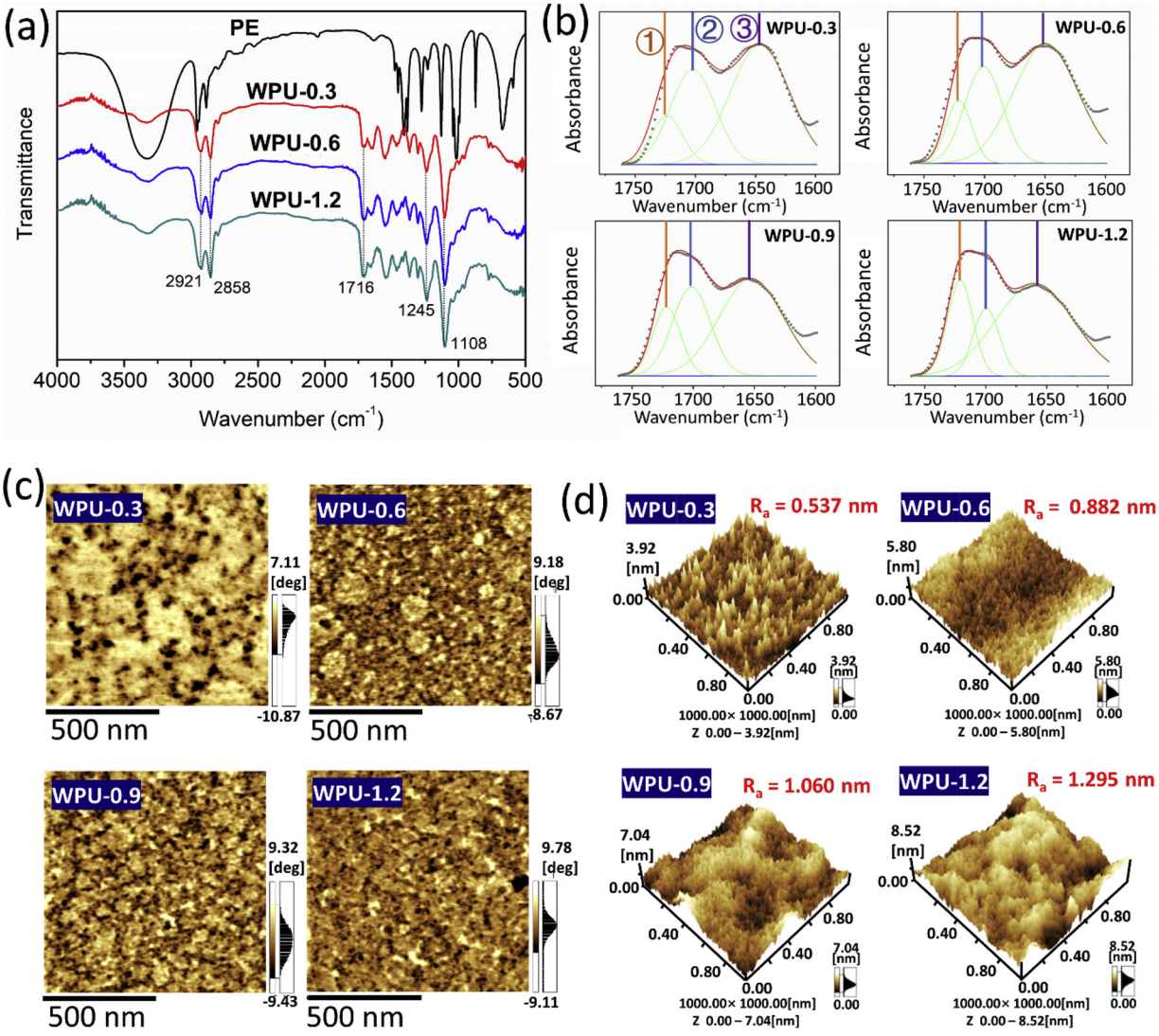

Fig. 2. (a) FTIR spectra of WPU coatings and (b) expansion area with fitting curves: ①free C = O at 1724 cm^{-1}, ②disordered C = O at 1700 cm^{-1}, ③ordered C = O at 1660-1630 cm^{-1}; (c) AFM phase images and (d) 3D height images of WPU coatings.

implying the crystallinity of hard segments. In comparison, WPU-0.6 and WPU-0.9 show a decreased intensity of bonded C═O while that of free C═O experiences an increase. Particularly, for WPU-1.2, peak intensity of free C═O is even higher than that of bonded C═O, indicating that incorporating PE had reduced chains interactions within hard segments. In other words, PE can increase cross-linkages of WPU coatings, causing soft segments to enter hard segment domains and be trapped in the hard segment domains. Thereby, the interactions between hard segments and soft segments are improved.

The microphase separation structure of WPU coatings were further investigated by AFM. Phase images obtained under force-tapping mode can provide information about energy dissipation between AFM tip and sample surface during measurement [32]. In this regard, it can tell the local stiffness difference of domains, thus allowing us to distinguish hard and soft phases in the samples. As shown in Fig. 2(c), phase images of WPU coatings have dark and bright areas which owing to soft segments and hard segments respectively [28]. For WPU-0.3, some dark spots resulted from aggregation of soft segment are distributed in domains where bright parts alternate with dark parts, indicating its distinct microphase separation structure. With progressively addition of PE, size of dark spots decreases, and its distribution become more evenly. Meanwhile, alternating boundary between dark area and bright area turn out to be blurred, implying enhanced interactions between soft segments and hard segments. These results are consisting with the FTIR results. 3D height images of coating surface were determined by AFM to intuitively show their surface morphology. As shown in Fig. 2(d), concave and convex regions are related to the soft segment and hard segment with different surface energy [33]. It can be seen intuitively that WPU coatings have different surface roughness (R_a). With increasing content of PE from 0.3% to 1.2%, R_a increased from 0.537 nm to 1.295 nm.

The process of latex film formation has several stages: as the water volatilizes, latex particles are closely packed, upon destruction of adsorption layer on surface of particles, the latex coalescence will occur, followed by the final intertwined and entangled of polymer chains [34]. After film formation is completed, some interparticle boundaries can also be observed [35,36]. The key to successful film formation is that temperature needs to be higher than minimum film formation temperature (MFFT), so that the deformation and cohesion of latex particles can occur to form consistent film. MFFT is regarded to be related to its glass transition temperature (T_g) [35]. Generally, MFFT is lower than the T_g of the corresponding polymer. Previous research has evidenced that T_g of PTMG based waterborne polyurethane is below 0 ℃ [5], hence, waterborne polyurethane in this study can form a film at room temperature. Since film formation involves stages from small particles to large particles to final film, more deformation and coalescence process will be involved with smaller the particles under equivalent WPU solid content. Thus, it is supposed that WPU dispersions with narrow particle size distribution would result in more interparticle boundaries during film-formation process, which may be one of the reasons for the increase in roughness. Even so, for all WPU samples, the altitude intercepts are below 10 nm, indicating coating surfaces are macroscopically smooth.

3.3. Physical properties of coatings formed by high solid content WPU

Hydrophilicity is one of important properties for coatings since it influences cleanability, durability and hand feeling of final product. As shown in Fig. 3(a1), water swelling ratio of WPU coatings increases with immersing time and reaches equilibrium after 65 min. It can be seen that WPU-0.6 and WPU-0.9 shows lower swelling ratio than WPU-0.3. This may because PE can work as chemical cross-linking point of molecular chains, which improves interaction between molecular chains to forms a compact network structure. As a result, stretching of flexible soft segment is restricted by rigid hard segment, limiting further penetrating of waters and volume expansion. Exceptional, WPU-1.2 exhibits higher water swelling ratio. Such phenomenon may be related to microphase structure of coatings since low crystalline region is disorderly and loosely arranged, which contribute to water absorption capacity. Mohan et al [37] has found that the swelling properties of polymer materials were influenced by crosslinking degree, functional groups, and synthesis conditions, etc. Hence, the value of swelling ratio is the result of combination of multiple elements. Generally, first-order kinetic equation can be applied to swelling process of water swellable elastomer with high initial swelling rate and ability to reach equilibrium quickly [38,39]. To investigate mechanism of swelling process of WPU coatings, a kinetic analysis with a first-order equation was conducted as shown below

$$dQ_t/dt = k(Q_e\text{-}Q_t) \quad (1)$$

where Q_t, Q_e and k denote the degree of swelling at any time, degree of swelling at equilibrium, and swelling rate constant, respectively. Integration of the Eq. (1) gives the following equation:

$$\ln(Q_e\text{-}Q_t) = \ln(Q_e\text{-}Q_0) - kt \quad (2)$$

Graphs were plotted against -ln (Qe - Qt) and t (Fig. 3(a2)) to examine the above kinetic model. Swelling rate constant (k) and can be obtained from the slope of the line while theoretical equilibrium swelling was calculated form intersection of the lines. The results are summarized in Table 3. It is showed that experimental results are close to theoretical data, which confirms that the swelling process of WPU coatings is consistent with kinetic first-order equation. Moreover, there is gradual increment in k, which may due to enhanced entanglement of soft segments and hard segments contributing to a low crystalline network, thus allowing water molecules to penetrate easily.

TGA can serve as a useful indicator of decomposition and flammability behavior of coatings [40]. The thermal stabilities of WPU coatings are shown in Fig. 3(b). There are two deposition stages where first stage from 270 ℃ to 380 ℃ is due to degradation of hard segments whilst the second stage from 380 ℃ to 500 ℃ is attributed to thermal decomposition of soft segments [5]. In comparison to PE which start to decomposition at 150 ℃, WPU-0.3 shows much higher thermal stability with a decomposition starting temperature (T_{-start}) at 283 ℃. It is noticed that T_{-start} of WPU-1.2 reaches 290 ℃, indicating the enhanced thermal stability. Generally, molecular chains break when temperature reaches a certain value. Polymer network with higher crosslinking contributes to the interaction force between polymer chains. In this regard, more heat is needed for mobility and breakage of molecular chains.

Mechanical property is another important evaluation criterion of coating performance. To applied on materials surface for finishing, coatings are supposed to possess both strength and flexibility to provide protection and extensibility. As shown in Fig. 3(c), the obtained strain-stress curves indicate that WPU samples exhibit breaking strength above 10 MPa, accompanying with elongation at break at around 400%, which indicating the toughness and flexibility of WPU coatings. In particular, strength at break of WPU coatings increases from 11.48 MPa to 14.70 MPa with increase of PE content whilst elongation at break reaches the highest value (431%) for WPU-0.3. This enhancement in mechanical strength may due to increased crosslinking in WPU molecular network result in higher toughness of WPU coatings.

Dynamic mechanical behavior of WPU coatings were also studied. Fig. 3(d1) and (d2) shows the results of storage modulus (E') and loss factor (tanδ) versus temperature. It can be seen that in the temperature region from -100 ℃ to 50 ℃, E′ for WPU coatings maintains at a high value. Besides, WPU-0.6 and WPU-1.2 has higher E′ than WPU-0.3, indicating their stronger restoring force after deformation, especially under daily use environment. Interestingly, upon temperature reaches 50 ℃, there is a turning point where E′ gradually decreases and presents a trend opposite to the low temperature region. The reason for this may be that PE increased the degree of network cross-linking, which means

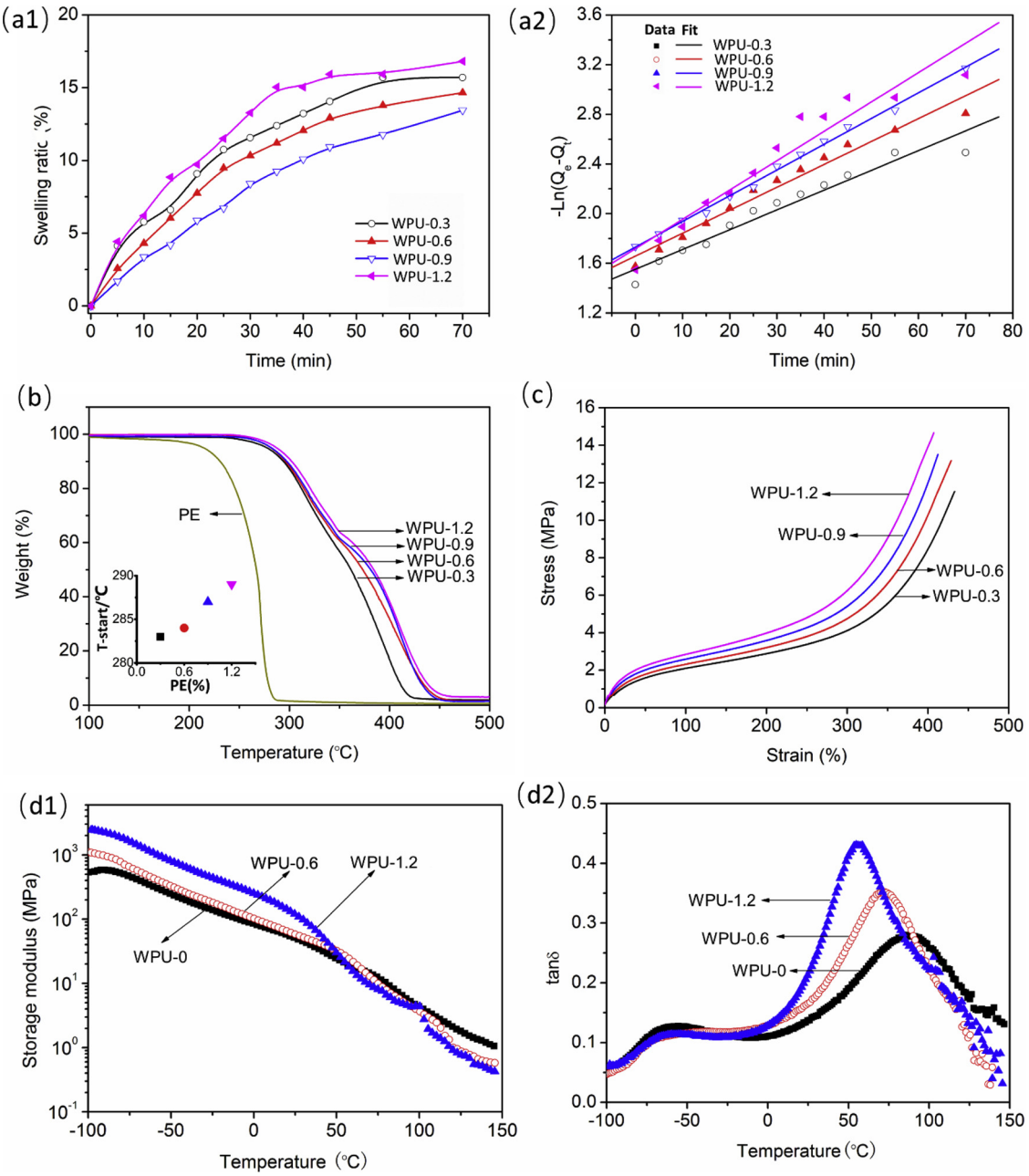

Fig. 3. (a1) water swelling ration of WPU coatings with respect to time; (a2) Pseudo-second-order kinetics of WPU coatings in water; (b) TGA curves of WPU coatings., (c) stress-strain curves, (d1) storage modulus E' and (d2) loss factor (tanδ) versus temperature.

Table 3
Parameters of swelling kinetics for WPU coatings.

Sample	Swelling ratio (%)		Rate constant k
	Calculated	Experimental	
WPU-0.3	21.2	21.5	0.0160
WPU-0.6	19.1	20.7	0.0184
WPU-0.9	17.7	17.6	0.0207
WPU-1.2	17.9	21.0	0.0236

that movement of soft molecular chains are limited by ambient rigid hard segments, hence, coatings behave as strong elastomer. As temperature gradually rises, hydrogen bonds between soft segment and hard segment begin to diminish, as a result, soft chains trapped in hard segment domains are able to move easily, leading to the enhanced ductility of coatings.

It can be seen in Fig. 3(d2), two distinct peaks of tanδ appears in low temperature region and the high temperature region, which indicates the microphase structure of WPU coatings. These two peaks correspond to glass transition of soft segments at low temperature and hard segments at high temperature [41]. Glass transition temperature of hard segments for WPU-0 and WPU-1.2 was 87.0 ℃ and 54.6 ℃, implying the lower crystallinity of hard segment for WPU-1.2. The peak values of tanδ indicate rate of mechanical dissipating energy which determined by movements of molecular chains in polymer and relative motions between each component in composites [42]. The higher the energy dissipation, the stronger the damping performance [41]. It is noticed that peak values of tanδ for WPU -0.6 and WPU-1.2 are higher than WPU-0. Particularly, tanδ for WPU-1.2 reaches is 0.44, almost twice that of WPU-0. Regarding to movement of the molecular chain inside WPU coatings, it may be proposed that as higher temperature (50 ℃),

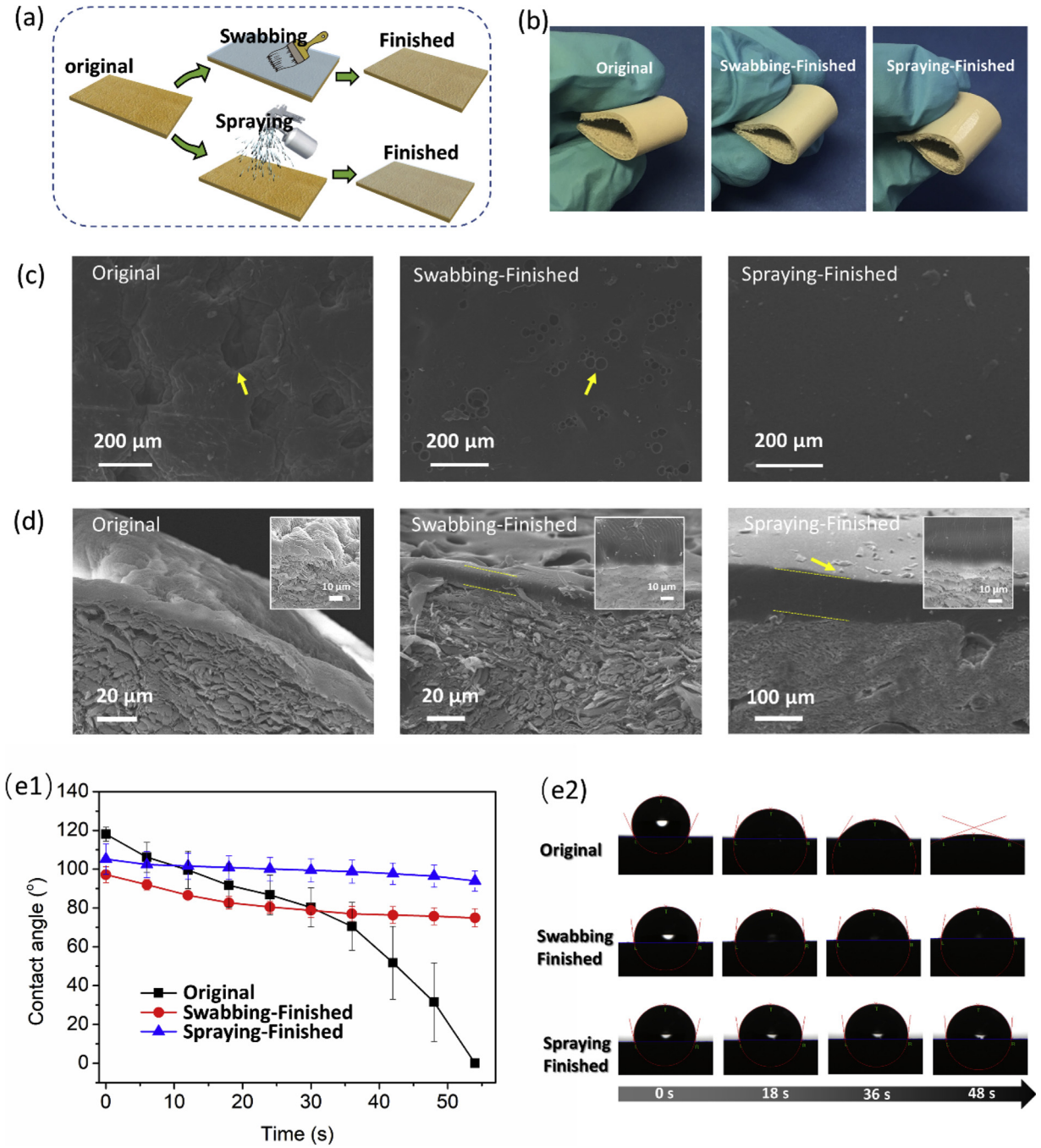

Fig. 4. (a) scheme of leather surface finishing processes including swabbing and spraying; (b) photos of original and finished leather; SEM images of (c) surface and (d) cross-section of original leather and finished leather, (e1) water contact angle of original and finished leather with respect to time; (e2) photos of variation in water contact angle as a function of corrosion time.

the soft segments entering the hard segment phase are released due to breakage of hydrogen bonds, which facilitates mobility of soft molecular chains and relative friction between hard segments and soft segments. In this way, more energy can be consumed to improve the damping performance of WPU coatings.

3.4. Application of high solid content on leather finishing

To evaluate applicability of high solid content WPU dispersions, WPU-0.6 dispersions was chosen as finishing agent to apply on leather by swabbing and spraying which are the most commonly used finishing methods [43]. The schemes of finishing processes are illustrated in Fig. 4(a). The leathers used for application were full grain white dyed calf leathers for bag production. Fig. 4(b) shows the photos of original leather and finished leather. Compares to original sample, finishing process resulted in glossy appearance and it was not observed any impairment on the limpness of leather. Moreover, finished leather can be distorted without delamination, which demonstrates applicability of WPU dispersions as leather finishing agent. Surface morphology of original and finished leather were characterized by SEM. As shown in Fig. 4(c), natural pore structure of leather can be observed. For swabbing-finished leather, there are some circular holes on the surface. These holes are formed during the painting process due to the less load of WPU dispersions. This void structure of coating is similar to the pore structure on surface of original leather, which is favorable for breathable and moisture permeable properties [44]. On the contrary, spraying

Table 4
Performance of WPU finished leather.

Item	Testing method	Swabbing finished leather	Spraying finished leather
Rubbing Fastness	In accordance with method DIN EN ISO 11640	4/5	4/5
Flexing endurance	In accordance with method DIN 53359	No change after 100,000 times flex	No change after 100,000 times flex
Gloss (60°)	Gloss meter	75	58
Breaking elongation	–	55.6%	63. 9%
Breaking strength	–	15.6 MPa	16.1 MPa

finished leather has smooth and void-free surface. SEM images of cross-section for three leather samples are shown Fig. 4(d). Original leather has a natural fibrous structure. As surface finishing agent, WPU are supposed to tightly adhere to papillary layer to ensure durability of leather. From the cross-section of finished leather, it can be seen that there is no obvious boundary and delamination of papillary layer and coating layer, indicating the good adhesion and filling property of WPU dispersions. The surface contact angles (CA) of original and finished leather were also evaluated. Results showed that CA of original leather gradually decreased with time due to its high hydrophilicity. As expected, finishing can significantly improve waterproofness of leather as the CA of both swabbing finished and spraying finished leather showed minor changes over time. Particularly, CA for spraying finished leather maintained above 90°, indicating its superior water resistance. Table 4 demonstrates other properties of the finished leather which verifies the excellent comprehensive performance of WPU coatings. Particularly, WPU coatings shows barely impairment to the mechanical properties of leather (Figure S1). In summary, it can be concluded that the obtained high solid content WPU dispersions satisfies application requirements of leather surface finishing agents.

4. Conclusions

Waterborne polyurethane dispersions were prepared based on star-shape prepolymer which was synthesized via arm-first approach using pentaerythritol as core. Solid content of WPU dispersion reached 45%. With PE content increasing from 0.3% to 1.2%, particle size in WPU dispersions presented in a decreasing trend, exhibiting transition from bimodal distribution to monomodal distribution, which may contribute to surface roughness of coatings formed by WPU dispersions. FTIR confirmed the obtained coatings were targeted product and revealed interactions between soft segments and hard segments through hydrogen bonds. AFM demonstrated micro-phase separation structure of WPU coatings with variation of surfaces roughness (R_a) which ranges from 0.537 nm to 1.295 nm with progressively addition of PE. Water swelling ratio of WPU coatings is below 17% and swelling process is consistent with kinetic first-order equation. Moreover, thermal stability of WPU coatings were improved due to increased crosslinking. WPU coatings also showed good mechanical properties with breaking strength reaching 15 MPa and elongation at break of 400%. In addition, it is found that obtained WPU coatings possess optimum damping properties at 50 °C which can be regulated by PE content. Most importantly, WPU coatings possess excellent comprehensive performance which indicates its applicability as leather finishing agents. This research may lead to development of more facile and green method for preparation of high solid content WPU which can be applied on coatings, adhesives and finishing agents.

Conflicts of interest

There are no conflicts to declare.

Acknowledgements

This work is supported by the National Natural Science Foundation of China (51373147 and 51673162), Hong Kong Innovation and Technology Support Program “Development of Calfskin Leather with High Elastic Recovery Performance” (RD/CRI/013/13) and Hong Kong PhD Fellowship (PF15-15110).

Appendix A. Supplementary data

Supplementary material related to this article can be found, in the online version, at doi:https://doi.org/10.1016/j.porgcoat.2019.01.031.

References

[1] J. Hu, K. Peng, J. Guo, D. Shan, G.B. Kim, Q. Li, E. Gerhard, L. Zhu, W. Tu, W. Lv, Click cross-linking-improved waterborne polymers for environment-friendly coatings and adhesives, ACS Appl. Mater. Interfaces 8 (2016) 17499–17510.
[2] H. Zhou, H. Wang, H. Niu, Y. Zhao, Z. Xu, T. Lin, A waterborne coating system for preparing robust, self-healing, superamphiphobic surfaces, Adv. Funct. Mater. 27 (2017) 1604261.
[3] S.Y. Kang, Z. Ji, L.F. Tseng, S.A. Turner, D.A. Villanueva, R. Johnson, A. Albano, R. Langer, Design and synthesis of waterborne polyurethanes, Adv. Mater. (2018).
[4] Y. Xiao, X. Fu, Y. Zhang, Z. Liu, L. Jiang, J. Lei, Preparation of waterborne polyurethanes based on the organic solvent-free process, Green Chem. 18 (2016) 412–416.
[5] Y. Han, J. Hu, Z. Xin, In-situ incorporation of alkyl-grafted silica into waterborne polyurethane with high solid content for enhanced physical properties of coatings, Polymers 10 (2018) 514.
[6] S.-h. Hsu, H.-J. Tseng, Y.-C. Lin, The biocompatibility and antibacterial properties of waterborne polyurethane-silver nanocomposites, Biomaterials 31 (2010) 6796–6808.
[7] E. Scrinzi, S. Rossi, F. Deflorian, C. Zanella, Evaluation of aesthetic durability of waterborne polyurethane coatings applied on wood for interior applications, Prog. Org. Coat. 72 (2011) 81–87.
[8] L. Lei, L. Zhong, X. Lin, Y. Li, Z. Xia, Synthesis and characterization of waterborne polyurethane dispersions with different chain extenders for potential application in waterborne ink, Chem. Eng. J. 253 (2014) 518–525.
[9] C.-K. Liu, N.P. Latona, G.L. DiMaio, Acoustic emission studies for leather coatings, J. Am. Leather Chem. Assoc. 97 (2002) 389–399.
[10] S. Lee, B. Kim, High solid and high stability waterborne polyurethanes via ionic groups in soft segments and chain termini, J. Colloid Interface Sci. 336 (2009) 208–214.
[11] H. Lijie, D. Yongtao, Z. Zhiliang, S. Zhongsheng, S. Zhihua, Synergistic effect of anionic and nonionic monomers on the synthesis of high solid content waterborne polyurethane, Colloids Surf. A Physicochem. Eng. Asp. 467 (2015) 46–56.
[12] Z. Zhu, R. Li, C. Zhang, S. Gong, Preparation and properties of high solid content and low viscosity waterborne polyurethane—acrylate emulsion with a reactive emulsifier, Polymers 10 (2018) 154.
[13] L. Bao, H. Fan, Y. Chen, J. Yan, J. Zhang, Y. Guo, Synthesis of 1, 4-Butanediol di (3-Diethylamino-2-Hydroxylpropyl alcohol) ether and cationic waterborne polyurethane with high solids content, Adv. Polym. Technol. 37 (2018) 906–912.
[14] D.H. Jung, E.Y. Kim, Y.S. Kang, B.K. Kim, High solid and high performance UV cured waterborne polyurethanes, Colloids Surf. A Physicochem. Eng. Asp. 370 (2010) 58–63.
[15] M. Li, F. Liu, Y. Li, X. Qiang, Synthesis of stable cationic waterborne polyurethane with a high solid content: insight from simulation to experiment, RSC Adv. 7 (2017) 13312–13324.
[16] A. Guyot, F. Chu, M. Schneider, C. Graillat, T. McKenna, High solid content latexes, Prog. Polym. Sci. 27 (2002) 1573–1615.
[17] S.-J. Peng, Y. Jin, X.-F. Cheng, T.-B. Sun, R. Qi, B.-Z. Fan, A new method to synthesize high solid content waterborne polyurethanes by strict control of bimodal particle size distribution, Prog. Org. Coat. 86 (2015) 1–10.
[18] R. Goseki, S. Ito, A. Hirao, Synthesis of multicomponent asymmetric star-branched polymers by iterative methodology with new diblock copolymer in-chain anions as building blocks, Polymer 124 (2017) 284–292.
[19] F. Snijkers, H.Y. Cho, A. Nese, K. Matyjaszewski, W. Pyckhout-Hintzen, D. Vlassopoulos, Effects of core microstructure on structure and dynamics of star polymer melts: from polymeric to colloidal response, Macromolecules 47 (2014) 5347–5356.
[20] C.P. Teng, K.Y. Mya, K.Y. Win, C.C. Yeo, M. Low, C. He, M.-Y. Han, Star-shaped polyhedral oligomeric silsesquioxane-polycaprolactone-polyurethane as biomaterials for tissue engineering application, NPG Asia Mater. 6 (2014) e142.

[21] S. Wang, Y. Zhou, B. Zhuang, P. Zheng, H. Chen, T. Zhang, H. Hu, D. Huang, Star-shaped amphiphilic block polyurethane with pentaerythritol core for a hydrophobic drug delivery carrier, Polym. Int. 65 (2016) 551–558.
[22] X. Yang, L. Wang, W. Wang, H. Chen, G. Yang, S. Zhou, Triple shape memory effect of star-shaped polyurethane, ACS Appl. Mater. Interfaces 6 (2014) 6545–6554.
[23] J. Yi, C. Huang, H. Zhuang, H. Gong, C. Zhang, R. Ren, Y. Ma, Degradable polyurethane based on star-shaped polyester polyols (trimethylolpropane and ε-caprolactone) for marine antifouling, Prog. Org. Coat. 87 (2015) 161–170.
[24] C. Lin, L. Xu, L. Huang, J. Chen, Y. Liu, Y. Ma, F. Ye, H. Qiu, T. He, S. Yin, Metal coordination stoichiometry controlled formation of linear and hyperbranched supramolecular polymers, Macromol. Rapid Commun. 37 (2016) 1453–1459.
[25] T.K. Cho, M.H. Chong, B.C. Chun, H.R. Kim, Y.-C. Chung, Structure-property relationship and shape memory effect of polyurethane copolymer cross-linked with pentaerythritol, Fibers Polym. 8 (2007) 7–12.
[26] V. Eychenne, Z. Mouloungui, A. Gaset, Total and partial erucate of pentaerythritol. Infrared spectroscopy study of relationship between structure, reactivity, and thermal properties, J. Am. Oil Chem. Soc. 75 (1998) 293–299.
[27] A.K. Mishra, D. Chattopadhyay, B. Sreedhar, K. Raju, FT-IR and XPS studies of polyurethane-urea-imide coatings, Prog. Org. Coat. 55 (2006) 231–243.
[28] Y. Han, Z. Chen, W. Dong, Z. Xin, Improved water resistance, thermal stability, and mechanical properties of waterborne polyurethane nanohybrids reinforced by fumed silica via in situ polymerization, High Perform. Polym. 27 (2015) 824–832.
[29] L. Bistričić, G. Baranović, M. Leskovac, E.G. Bajsić, Hydrogen bonding and mechanical properties of thin films of polyether-based polyurethane–silica nanocomposites, Eur. Polym. J. 46 (2010) 1975–1987.
[30] D. Chattopadhyay, A.K. Mishra, B. Sreedhar, K. Raju, Thermal and viscoelastic properties of polyurethane-imide/clay hybrid coatings, Polym. Degrad. Stab. 91 (2006) 1837–1849.
[31] H.S. Lee, Y.K. Wang, S.L. Hsu, Spectroscopic analysis of phase separation behavior of model polyurethanes, Macromolecules 20 (1987) 2089–2095.
[32] P. Schön, K. Bagdi, K. Molnár, P. Markus, B. Pukánszky, G.J. Vancso, Quantitative mapping of elastic moduli at the nanoscale in phase separated polyurethanes by AFM, Eur. Polym. J. 47 (2011) 692–698.
[33] B. Gong, C. Ouyang, Y. Yuan, Q. Gao, Synthesis and properties of a millable polyurethane elastomer with low halloysite nanotube content, RSC Adv. 5 (2015) 77106–77114.
[34] A. Du Chesne, A. Bojkova, J. Gapinski, D. Seip, P. Fischer, Film formation and redispersion of waterborne latex coatings, J. Colloid Interface Sci. 224 (2000) 91–98.
[35] P. Berce, S. Skale, M. Slemnik, Electrochemical impedance spectroscopy study of waterborne coatings film formation, Prog. Org. Coat. 82 (2015) 1–6.
[36] J. Li, W. Zheng, W. Zeng, D. Zhang, X. Peng, Structure, properties and application of a novel low-glossed waterborne polyurethane, Appl. Surf. Sci. 307 (2014) 255–262.
[37] Y.M. Mohan, P.K. Murthy, K.M. Raju, Synthesis, characterization and effect of reaction parameters on swelling properties of acrylamide–sodium methacrylate superabsorbent copolymers, React. Funct. Polym. 63 (2005) 11–26.
[38] H. Schott, Swelling kinetics of polymers, J. Macromol. Sci. B: Phys. 31 (1992) 1–9.
[39] N. Mulye, S. Turco, A simple model based on first order kinetics to explain release of highly water soluble drugs from porous dicalcium phosphate dihydrate matrices, Drug Dev. Ind. Pharm. 21 (1995) 943–953.
[40] H.-B. Chen, P. Shen, M.-J. Chen, H.-B. Zhao, D.A. Schiraldi, Highly efficient flame retardant polyurethane foam with alginate/clay aerogel coating, ACS Appl. Mater. Interfaces 8 (2016) 32557–32564.
[41] T. Wang, S. Chen, Q. Wang, X. Pei, Damping analysis of polyurethane/epoxy graft interpenetrating polymer network composites filled with short carbon fiber and micro hollow glass bead, Mater. Des. 31 (2010) 3810–3815.
[42] S. Chen, Q. Wang, T. Wang, Damping, thermal, and mechanical properties of montmorillonite modified castor oil-based polyurethane/epoxy graft IPN composites, Mater. Chem. Phys. 130 (2011) 680–684.
[43] T. Tysak, Low gloss aqueous coating compositions containing poly (ethylene oxide) for use on leather, in, Google Patents, 2015.
[44] Y. Wu, A. Wang, R. Zheng, H. Tang, X. Qi, B. Ye, Laser-drilled micro-hole arrays on polyurethane synthetic leather for improvement of water vapor permeability, Appl. Surf. Sci. 305 (2014) 1–8.